Cover Sheet

Corresponding Author: Mathieu Van Eeckhaute;
Phone: +3226502857;
Email: mveeckha@ulb.ac.be

Low Complexity Iterative Localization of Time-Misaligned Terminals in Cellular Networks

Mathieu Van Eeckhaute, Thomas Van der Vorst, André Bourdoux, François Quitin,
Philippe De Doncker and François Horlin

Abstract—Recently, iterative localization has arisen as a promising approach to localize a Mobile Station (MS) in a cellular system. The conventional geo-location is obtained in a two-step approach: propagation delays are estimated and then the multi-lateration is responsible for the determination of the user position, based on the estimated delays. Iterative localization iterates between the two conventional steps to progressively refine delay estimates based on the position estimate available from the previous iterations. This localization scheme was seen to provide appealing performances compared to the two-step approach. It also seems to be computationally attractive with respect to direct localization that estimates the position using the digitized received signals directly. However, the iterative localization solution developed in literature relies on a strict time synchronization between MS and Base Stations (BSs). Moreover, the computational complexity of the iterative approach is not thoroughly compared to two-step and optimal solutions. This paper therefore proposes a new iterative localization method able to operate in a cellular system with time-misaligned terminals. We show by means of a detailed complexity analysis that the iterative positioning algorithm is one order of magnitude less complex than direct localization. Simulation results prove that the achievable performance after a few iterations approaches the performance of the direct localization solution.

Index Terms—Iterative localization, direct positioning estimation, performance/complexity analysis.

I. INTRODUCTION

In addition to the communication functionality, cellular networks are evolving towards increasingly accurate geo-location services [1]. In 2G and 3G, the Mobile Station (MS) location is determined based on Enhanced Cell ID (E-CID) that refines the location information obtained from the Cell ID with the estimate of the Round Trip Time (RTT) and the Received Signal Strength (RSS). The spatial resolution of this method does not exceed 100 meters. The provided position estimate is therefore mainly used to accelerate the initialization phase of the more accurate Global Navigation Satellite System (GNSS) positioning. Further on, 4G includes

a specific Positioning Reference Signal (PRS) in its protocol to allow a fine estimation of the signal Time-of-Arrival (ToA). This PRS is defined as an Orthogonal Frequency Division Multiplexing (OFDM) signal spread in time and frequency [2].

Localization methods based on the ToA rely on the estimation of the absolute time-of-flight between the source and the receiver. The MS must be strictly time synchronized to the Base Stations (BSs). In practice, the quality of the backbone network allows to synchronize the BSs together but the time offset of the MS often remains unknown. Estimated ToAs are therefore affected by a common time offset. The transmitter position can then be estimated together with the time offset by working with the estimated ToAs directly. Another solution is to eliminate the unknown time offset by defining a set of Time Difference of Arrivals (TDoAs) from the estimated ToAs.

The conventional two-step approach to localize a source first estimates ToAs/TDoAs using the received signals. The position of the MS is then determined in a multi-lateration step where the non-linear system of equations formed by the ToA/TDoA estimates is solved. A lot of algorithms have been developed in literature to perform this multi-lateration. They can work on the non-linear equations like the Maximum Likelihood (ML) estimator developed in [3]. This estimator jointly estimates the position and the time offset of the user from the ToA estimates. Paper [4] rather proposes an ML estimator working with TDoAs extracted from the ToA estimations. Localization algorithms can also work on linearized equations like in [5], [6] for TDoA and in [7] for ToA formulations.

One of the main causes of inaccuracies in ToA-based cellular localization systems is multipath propagation. In urban environments, Line-of-Sight (LOS) condition can often not be guaranteed between the MS and all the BSs involved in the localization process. Non Line-of-Sight (NLOS) conditions introduce a bias in the ToAs observed at the BSs [8]. In two-step positioning, multipath propagation can be alleviated at both delay estimation and multi-lateration steps. The delay estimation generally consists in estimating the ToA of the first arrival path. This can be done using the Generalized Maximum Likelihood approach of [9] which jointly estimates all multipath coefficients and their arrival times in an iterative manner. Another approach is the frequency domain super-resolution ToA estimation of [10] and [11]. Those subspace methods use an estimation of the signal autocorrelation which requires a large number of independent signal observations with the same ToA. The authors of [12] and [13] rather rely on the central limit theorem for random vectors to formulate an ML ToA estimator in dense multipath. They show that based

Mathieu Van Eeckhaute, François Quitin, Philippe de Doncker and François Horlin are with the Université libre de Bruxelles, 1050 Brussels, Belgium (e-mail: {mveeckha, fquitin, pdedonck, fhorlin}@ulb.ac.be)

Thomas Van der Vorst is with the Université libre de Bruxelles, 1050 Brussels, Belgium and with the Sorbonne Université, L2E, F-75005 Paris, France (e-mail: tvdvorst@ulb.ac.be)

André Bourdoux is with the Inter-university Micro-Electronics Center (IMEC), Kapeldreef 75, 3008 Leuven, Belgium (e-mail:bourdoux@imec.be)

on some prior knowledge on the shape of the channel power delay profile their estimator outperforms super-resolution and GML approaches in a practical indoor environment. Due to the blockage of direct path, the ToA of the first path may be affected by a positive bias. A comprehensive survey of the main NLOS mitigation techniques in the multi-lateration step is provided in [14] and references therein. While most of the NLOS mitigation techniques in [14] require prior information on NLOS errors, [15] more recently proposed a NLOS multi-lateration algorithm for Wireless Sensor Networks able to operate without any prior information on NLOS errors. The latter method does not discard the NLOS range measurements and relaxes the localization problem using semi-definite programming (SDP) to limit the implementation complexity.

Another methodology to estimate the user position is the Direct Position Estimation (DPE) proposed in papers [16] and [17]. While conventional two-step location systems require ToA/TDoA estimates to geometrically solve user coordinates, DPE directly estimates the position coordinates from the digitized received signals. Paper [18] analytically demonstrates that the two-step approach cannot overcome DPE while [19] shows by simulations that DPE provides an important performance gain compared to the two-step method, especially for lower Signal-to-Noise Ratios (SNRs). DPE algorithms proposed in literature rely on the optimization of a multi-variate non-convex cost function, like the ML estimator proposed in [16]. Although outperforming the two-step approach, this method suffers from a significant complexity increase. Digitized received signals also need to be transmitted to the fusion center. This incurs a lot of communication overhead.

At the time of writing, there is only a few DPE algorithms designed to operate with a frequency-selective multipath environment. Authors of [20] develop an Angle of Arrival (AoA) based DPE method working with frequency-selective channels but assuming strong LOS propagation. Paper [21] recently introduced a joint ToA-AoA DPE technique operating with an arbitrary multipath channel. The algorithm works with OFDM signals and relies on a subspace method to limit the computational load. However, the latter approach needs a large number of signal observations and requires to estimate the location of the scatterers.

An intermediate approach between two-step and direct positioning is proposed in [22]. Instead of transmitting the received signal to the fusion center as in DPE, each BS only sends the sufficient statistics (sample covariance matrix) to estimate the position at the fusion center. This method has only been developed for Angle-of-Arrival based positioning using narrowband signals received by antenna arrays at the BSs. Paper [22] relies on the Multiple Signal Classification (MUSIC) algorithm to derive the user position. Authors of [23] rather perform the localization from the correlation matrices using the Method-Of-Direction Estimation (MODE) algorithm that is more robust to correlation in the received signals.

We recently demonstrated that the performance of the DPE can be approached by iterating between the two conventional steps (ToA estimate and multi-lateration) [24]. To the best knowledge of the authors, there exists no other comparable iteration-based localization method in literature. The algorithm makes use of the Bayes framework to take into account prior knowledge on the statistics obtained from the previous iterations. Information exchanged between the delay estimation and position estimation steps consists of the means and variances of delay and position estimates. However, our original work unrealistically assumed the MS to be strictly synchronized to the BSs and did not include any computational complexity analysis.

Contributions: The contributions of this paper can be summarized as follows:

- We propose an iterative positioning algorithm able to localize a MS affected by an unknown time offset. The proposed position estimation step jointly determines the user coordinates and the time offset based on the ToA measurements from the delay estimation step. Those position and time offset estimates are used as prior information for the next iteration.
- We show the computational savings achieved by the iterative formulation compared to DPE by means of a detailed complexity analysis.
- We illustrate the performance of the developed algorithms using numerical simulations. We focus on an emerging cellular scenario making use of the OFDM modulation in a network composed of small cells with strictly synchronized base stations. We assess the impact of multipath propagation on our algorithm in a LOS and obstructed LOS scenario.

The rest of the paper is organized as follows. Section II introduces the OFDM signal model. A description of the iterative positioning algorithm is provided in Section III. The complexity of the considered localization schemes is analyzed in Section IV. Section V numerically assesses the complexity and the performance compared to state-of-the-art DPE and two-step approaches.

Throughout the text, vectors and matrices are identified by lowercase and uppercase bold letters respectively. The real part operator is represented by $\Re\{\}$. Expression $\text{diag}(\mathbf{x})$ represents a diagonal matrix with elements of vector $\mathbf{x}$ on the diagonal. The ith element of vector $\mathbf{x}$ is denoted by x_i while a vector containing all elements of $\mathbf{x}$ excepting the kth one is written as $\mathbf{x}^k$.

II. SYSTEM MODEL

We consider a cellular network operating with OFDM modulation. For the sake of clarity, we focus on the uplink, but the discussion can easily be extended to the downlink as long as BSs transmit orthogonal signals. The MS is simultaneously connected to K neighbouring time-synchronized BSs and operates on a communication bandwidth B centered around the carrier frequency f_c. The OFDM modulation splits the communication bandwidth in Q orthogonal sub-carriers allocated to data or pilot symbols. A cyclic prefix (CP) is inserted in each multi-carrier block. This CP allows to maintain orthogonality among the sub-carriers when the signal undergoes a time dispersive channel.

For the sake of simplicity, we assume a single path Line-Of-Sight (LOS) channel introducing a delay τ_k between the MS

and the kth BS. Delay $\tau_k(x,y) = d_k(x,y)/c$ is the time-of-flight of the signal with $d_k(x,y) = \sqrt{(x-x_k)^2 + (y-y_k)^2}$ and c being the speed of light. Coordinates $\{x,y\}$ and $\{x_k, y_k\}$ respectively denote the position of the MS and of the kth base station.

The received OFDM signal is affected by a time offset and a carrier frequency offset (CFO) that are roughly estimated before the positioning takes place. This is achieved using the preamble sequences appearing at the beginning of each frame in typical OFDM-like communication systems [25]. The rough synchronization leaves a remaining CFO that can be approximated as a common phase offset affecting all sub-carriers in a given multi-carrier block. There is also a remaining time offset t_k that falls within the cyclic prefix. As all BSs are perfectly time synchronized, the remaining time offset t_k can be expressed as

$$t_k(x,y,t_0) = \tau_k(x,y) + t_0 \tag{1}$$

where t_0 is the common time offset between the MS and the BSs. Multiplying expression (1) by the speed of light gives the pseudorange observed at BS k

$$\delta_k(x,y,t_0) = d_k(x,y) + \delta_0 \tag{2}$$

where $\delta_0 = ct_0$ is the range offset.

Considering that the time-of-arrival $t_k(x,y,t_0)$ is shorter than the CP duration, sub-carriers remain orthogonal and the frequency domain signal received on sub-carrier q at BS k is given for one OFDM block by

$$r_{kq} = a_k e^{j\phi_k} s_q e^{-j2\pi \frac{q\delta_k(x,y,t_0)}{QT_c}} + w_{kq} \tag{3}$$

for $q = -Q/2, ..., Q/2 - 1$ and $k = 1, ..., K$. Symbol s_q can either carry data or be a pilot symbol, $T = 1/B$ is the sample period and a_k models the signal amplitude. The term w_{kq} is the Additive White Gaussian Noise (AWGN) of variance $\sigma_{w_k}^2$ affecting sub-carrier q at BS k. The variance of this AWGN is assumed to be known at the receiver.

Base station k then estimates the pseudorange $\delta_k(x,y,t_0)$ by observing model (3) on the subset of pilot sub-carriers $\mathcal{P} = \{q_1, ..., q_P\}$ reserved for positioning. Since the pseudorange is estimated using positioning pilot sub-carriers of a single OFDM block, the channel can be assumed constant during the localization process.

By gathering received signals on pilot sub-carriers, we can build an equivalent vector model

$$\mathbf{r}_k = a_k e^{j\phi_k} \mathbf{s}(\delta_k) + \mathbf{w}_k \tag{4}$$

where

$$\mathbf{r}_k = [r_{kq_1}, ..., r_{kq_P}]^T \tag{5}$$

$$\mathbf{w}_k = [w_{kq_1}, ..., w_{kq_P}]^T \tag{6}$$

and

$$\mathbf{s}(\delta_k) = [s_{q_1} e^{-j2\pi \frac{q_1 \delta_k}{QT_c}}, ..., s_{q_P} e^{-j2\pi \frac{q_P \delta_k}{QT_c}}]^T \tag{7}$$

with δ_k standing for $\delta_k(x,y,t_0)$.

Pilot sub-carriers considered to estimate the pseudorange in this paper are used in nowadays cellular systems for ToA
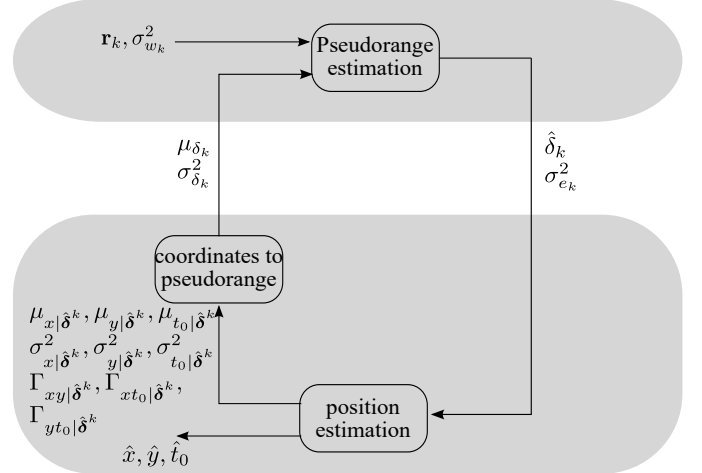

Fig. 1. Iterative Delay/Position Estimation.

estimation. For example in LTE, such frequency domain pilot symbols are the Sounding Reference Signals (SRS) in uplink and the Positioning Reference Signal (PRS) in downlink [2].

III. ITERATIVE POSITIONING

The proposed positioning system extends the framework developed in [24] to a scenario in which the MS is not strictly time synchronized to the BSs. The working principle of the iterative algorithm is illustrated in Fig. 1.

In uplink, two implementations of the algorithm can be considered in backhaul cellular systems. The pseudorange estimation step can be implemented at the base stations. Those base stations would then transfer the pseudorange estimates and their reliability to a fusion center (similar to the LTE Evolved Serving Mobile Location Center) that implements the multi-lateration [26, chap. 2]. Antenna sites can alternatively directly transfer their baseband signals to the fusion center that would then implement both pseudorange estimation and multi-lateration steps. Exchanges between base stations and fusion center involved in the first implementation would introduce a 10ms delay at each iteration [26, chap. 2]. While not introducing additional delay, the second implementation would require a high capacity backhaul between the antenna sites and the baseband processing unit, like optical fibers linking the remote radio heads and the baseband unit in a 3GPP distributed antenna Coordinated Multi-Point (CoMP) system [26, chap. 12]. Our positioning algorithm can also be implemented in downlink as long as BSs transmit orthogonal signals. In this case the mobile station implements both pseudorange and position estimation steps.

A. Pseudorange Estimation

One independent pseudorange measurement is made per base station. The prior information received on the pseudorange (estimate and reliability of this estimate) is refined using the pilot sub-carriers of the received OFDM signal. Resorting

to the Bayes framework [27], the posterior Probability Density Function (PDF) of δ_k can be obtained as follows

$$p(\delta_k|\mathbf{r}_k) = \frac{p(\mathbf{r}_k|\delta_k)p(\delta_k)}{\int\limits_{-\infty}^{+\infty} p(\mathbf{r}_k|\delta_k)p(\delta_k)d\delta_k}. \tag{8}$$

Similar to [24], we assume that the observed pseudorange δ_k has a Gaussian prior PDF characterized by its mean μ_{δ_k} and its variance $\sigma_{\delta_k}^2$

$$p(\delta_k) = C_{\delta_k} \exp\left(-\frac{1}{2\sigma_{\delta_k}^2}\left(\delta_k - \mu_{\delta_k}\right)^2\right) \tag{9}$$

where C_{δ_k} is a constant. We also know from (4) that the received signal $\mathbf{r}_k$ follows a Gaussian distribution

$$p(\mathbf{r}_k|\delta_k, a_k, \phi_k) = C_{r_k} \exp\left(-\frac{1}{\sigma_{w_k}^2}\left(\mathbf{r}_k - a_k e^{j\phi_k}\mathbf{s}(\delta_k)\right)^H \right. $$
$$\left. \cdot \left(\mathbf{r}_k - a_k e^{j\phi_k}\mathbf{s}(\delta_k)\right)\right) \tag{10}$$

where C_{r_k} is a constant.

The PDF $p(\mathbf{r}_k|\delta_k)$ in (8) is obtained from (10) by marginalizing the nuisance parameters a_k and ϕ_k

$$p(\mathbf{r}_k|\delta_k) = \int\limits_{-\infty}^{+\infty}\int\limits_{-\infty}^{+\infty} p(\mathbf{r}_k|\delta_k, a_k, \phi_k)p(a_k)p(\phi_k)da_k d\phi_k. \tag{11}$$

The final exression of the posterior delay distribution is given in (12). The latter expression is obtained by substituting expressions (9) - (11) in (8) and simplifying terms that do not depend on δ_k, a_k or ϕ_k.

Computing the mean and the variance of the pseudorange knowing the latter posterior PDF provides the Minimum Mean Square Error (MMSE) estimation $\hat{\delta}_k$ together with its reliability [27]

$$\hat{\delta}_k = \int\limits_{-\infty}^{+\infty} \delta_k \; p(\delta_k|\mathbf{r}_k)d\delta_k \tag{13}$$

$$\sigma_{e_k}^2 = \int\limits_{-\infty}^{+\infty} (\delta_k - \hat{\delta}_k)^2 p(\delta_k|\mathbf{r}_k)d\delta_k \tag{14}$$

where $e_k = \delta_k - \hat{\delta}_k$ can be seen as the pseudorange estimation error.

B. Joint Position and Synchronization Estimation

The fusion center makes one independent estimation per base station. For each base station, the position of the MS is deduced from the pseudorange estimates of the $K-1$ other BSs. Excluding the current BS ensures the independence of the prior information communicated to the time-of-arrival estimation step in the next iteration with the signal received at the base station. This implies that our algorithm requires at least four BSs to jointly synchronize and localize a MS in the 2D plane. The error e_k corrupting the observed pseudorange at base station k is assumed to be Gaussian distributed of zero

mean and variance $\sigma_{e_k}^2$. The pseudorange observed at BS k reads

$$\hat{\delta}_k = \delta_k(x, y, t_0) + e_k \tag{15}$$

We can build an equivalent vector model used to compute the position estimate at base station k by gathering the observed pseudoranges from the $K-1$ other BSs

$$\hat{\boldsymbol{\delta}}^k = \boldsymbol{\delta}^k(x, y, t_0) + \boldsymbol{e}^k \tag{16}$$

where

$$\hat{\boldsymbol{\delta}}^k = [\hat{\delta}_1, ..., \hat{\delta}_{k-1}, \hat{\delta}_{k+1}, ..., \hat{\delta}_K]^T \tag{17}$$
$$\boldsymbol{\delta}^k(x, y, t_0) = [\delta_1(x, y, t_0), ..., \delta_{k-1}(x, y, t_0),$$
$$\delta_{k+1}(x, y, t_0), ..., \delta_K(x, y, t_0)]^T \tag{18}$$
$$\boldsymbol{e}^k = [e_1, ..., e_{k-1}, e_{k+1}, ..., e_K]^T. \tag{19}$$

Note that the index of the target base station is absent in those vector expressions.

Elements of $\boldsymbol{e}^k$ are independent and of possibly different variance since the reliability of the distance estimations can depend on the base station index. The noise covariance matrix is therefore diagonal and given by

$$\mathbf{C}_{\boldsymbol{e}^k} = \mathrm{diag}\left([\sigma_{e_1}^2, ..., \sigma_{e_{k-1}}^2, \sigma_{e_{k+1}}^2, ..., \sigma_{e_K}^2]\right). \tag{20}$$

The position estimate from base station k and its reliability are obtained using the posterior PDF of the position given the pseudorange estimations of the $K-1$ other BSs. We assume coordinates x and y to be uniformly distributed on intervals $[x_{\min}, \; x_{\max}]$ and $[y_{\min}, \; y_{\max}]$. The time offset t_0 is also considered to be uniformly distributed on $[t_{0_{\min}}, \; t_{0_{\max}}]$ and is independent from the user position. The posterior PDF of the user position is thus expressed by

$$p(\boldsymbol{\gamma}|\hat{\boldsymbol{\delta}}^k) = \frac{p(\hat{\boldsymbol{\delta}}^k|\boldsymbol{\gamma})p(\boldsymbol{\gamma})}{\int\limits_{-\infty}^{+\infty} p(\hat{\boldsymbol{\delta}}^k|\boldsymbol{\gamma})p(\boldsymbol{\gamma})d\boldsymbol{\gamma}} \tag{21}$$

where $\boldsymbol{\gamma}$ gathers variables x, y and t_0, i.e. $\boldsymbol{\gamma} = [x, y, t_0]^T$. We therefore have that

$$p(\boldsymbol{\gamma}) = \begin{cases} \left(\prod_{l=1}^3 \gamma_{l,\max} - \gamma_{l,\min}\right)^{-1} & \boldsymbol{\gamma}_{\min} \leq \boldsymbol{\gamma} \leq \boldsymbol{\gamma}_{\max} \\ 0 & \text{otherwise} \end{cases} \tag{22}$$

where $\boldsymbol{\gamma}_{\min} = [x_{\min}, y_{\min}, t_{0_{\min}}]^T$ and $\boldsymbol{\gamma}_{\max} = [x_{\max}, y_{\max}, t_{0_{\max}}]^T$ From (16), we know that the PDF $p(\hat{\boldsymbol{\delta}}^k|\boldsymbol{\gamma})$ is Gaussian distributed, i.e.

$$p(\hat{\boldsymbol{\delta}}^k|\boldsymbol{\gamma}) = C_k \exp\left(-\frac{1}{2}\left(\hat{\boldsymbol{\delta}}^k - \boldsymbol{\delta}^k(\boldsymbol{\gamma})\right)^T \mathbf{C}_{\boldsymbol{e}^k}^{-1}\left(\hat{\boldsymbol{\delta}}^k - \boldsymbol{\delta}^k(\boldsymbol{\gamma})\right)\right) \tag{23}$$

where C_k is a constant.

Inserting expression (23) in (21) and remembering that $\boldsymbol{\gamma}$ follows the uniform distribution (22) yields after simplification of the terms independent from $\boldsymbol{\gamma}$ that

$$p(\delta_k|\mathbf{r}_k) = \frac{\left(\int_{-\infty}^{+\infty} \int_{-\infty}^{+\infty} \exp\left(\frac{2}{\sigma_{w_k}^2} a_k \cos\phi_k \Re\{\mathbf{r}_k^H \cdot \mathbf{s}(\delta_k)\} - a_k^2 P\right) p(a_k)p(\phi_k) da_k d\phi_k \right) \cdot \exp\left(\frac{1}{\sigma_{\delta_k}^2}(\mu_{\delta_k}\delta_k - \frac{\delta_k^2}{2})\right)}{\int_{-\infty}^{+\infty} \left(\int_{-\infty}^{+\infty} \int_{-\infty}^{+\infty} \exp\left(\frac{2}{\sigma_{w_k}^2} a_k \cos\phi_k \Re\{\mathbf{r}_k^H \cdot \mathbf{s}(\delta_k)\} - a_k^2 P\right) p(a_k)p(\phi_k) da_k d\phi_k \right) \cdot \exp\left(\frac{1}{\sigma_{\delta_k}^2}(\mu_{\delta_k}\delta_k - \frac{\delta_k^2}{2})\right) d\delta_k}. \tag{12}$$

$$p(\boldsymbol{\gamma}|\hat{\boldsymbol{\delta}}^k) = \begin{cases} \dfrac{\exp\left(\left(\hat{\boldsymbol{\delta}}^k - \frac{1}{2}\boldsymbol{\delta}^k(\gamma)\right)^T \cdot \mathbf{C}_{e^k}^{-1} \cdot \boldsymbol{\delta}^k(\gamma) \right)}{\int_{\gamma_{\min}}^{\gamma_{\max}} \exp\left(\left(\hat{\boldsymbol{\delta}}^k - \frac{1}{2}\boldsymbol{\delta}^k(\gamma)\right)^T \cdot \mathbf{C}_{e^k}^{-1} \cdot \boldsymbol{\delta}^k(\gamma) \right) d\gamma} . & \gamma_{\min} \leq \gamma \leq \gamma_{\max} \\ \\ 0 & \text{otherwise} \end{cases} \tag{24}$$

The MMSE estimate of $\boldsymbol{\gamma}$ is given by the mean vector $\boldsymbol{\mu}_{\boldsymbol{\gamma}|\hat{\boldsymbol{\delta}}^k} = \left[\mu_{x|\hat{\boldsymbol{\delta}}^k}, \mu_{y|\hat{\boldsymbol{\delta}}^k}, \mu_{t_0|\hat{\boldsymbol{\delta}}^k} \right]^T$ that can be obtained as

$$\boldsymbol{\mu}_{\boldsymbol{\gamma}|\hat{\boldsymbol{\delta}}^k} = \int_{\gamma_{\min}}^{\gamma_{\max}} \boldsymbol{\gamma}\, p(\boldsymbol{\gamma}|\hat{\boldsymbol{\delta}}^k) d\boldsymbol{\gamma}. \tag{25}$$

The reliability of the estimate of $\boldsymbol{\gamma}$ is associated to the covariance matrix

$$\mathbf{C}_{\boldsymbol{\gamma}|\hat{\boldsymbol{\delta}}^k} = \begin{bmatrix} \sigma_{x|\hat{\boldsymbol{\delta}}^k}^2 & \Gamma_{xy|\hat{\boldsymbol{\delta}}^k} & \Gamma_{xt_0|\hat{\boldsymbol{\delta}}^k} \\ \Gamma_{xy|\hat{\boldsymbol{\delta}}^k} & \sigma_{y|\hat{\boldsymbol{\delta}}^k}^2 & \Gamma_{yt_0|\hat{\boldsymbol{\delta}}^k} \\ \Gamma_{xt_0|\hat{\boldsymbol{\delta}}^k} & \Gamma_{yt_0|\hat{\boldsymbol{\delta}}^k} & \sigma_{t_0|\hat{\boldsymbol{\delta}}^k}^2 \end{bmatrix}. \tag{26}$$

This matrix computes

$$\mathbf{C}_{\boldsymbol{\gamma}|\hat{\boldsymbol{\delta}}^k} = \int_{\gamma_{\min}}^{\gamma_{\max}} (\boldsymbol{\gamma} - \boldsymbol{\mu}_{\boldsymbol{\gamma}|\hat{\boldsymbol{\delta}}^k})(\boldsymbol{\gamma} - \boldsymbol{\mu}_{\boldsymbol{\gamma}|\hat{\boldsymbol{\delta}}^k})^T p(\boldsymbol{\gamma}|\hat{\boldsymbol{\delta}}^k) d\boldsymbol{\gamma}. \tag{27}$$

The MMSE estimate of $\boldsymbol{\gamma}$ for the current iteration is obtained from the average of the estimates acquired by the K BSs

$$\hat{\boldsymbol{\gamma}} = \frac{1}{K} \sum_{k=1}^{K} \boldsymbol{\mu}_{\boldsymbol{\gamma}|\hat{\boldsymbol{\delta}}^k}. \tag{28}$$

C. Position to Pseudorange Conversion

As explained in Section III-A, the pseudorange estimation step of the next iteration requires the knowledge of the mean and variance of the prior distribution of the observed pseudorange. Those two first order moments can be computed knowing the mean vector $\boldsymbol{\mu}_{\boldsymbol{\gamma}|\hat{\boldsymbol{\delta}}^k}$ and covariance matrix $\mathbf{C}_{\boldsymbol{\gamma}|\hat{\boldsymbol{\delta}}^k}$. However, relationships between $\boldsymbol{\gamma}$ and the pseudoranges are non-linear. In order to ease the computations, we perform a linear approximation around the mean to obtain closed form expressions. This makes sense since elements of the covariance matrix $\mathbf{C}_{\boldsymbol{\gamma}|\hat{\boldsymbol{\delta}}^k}$ are generally small. We can therefore approximate the pseudorange by its first order expansion around its mean

$$\begin{aligned} \delta_k(x, y, t_0) &\approx \delta_k(\mu_{x|\hat{\boldsymbol{\delta}}^k}, \mu_{y|\hat{\boldsymbol{\delta}}^k}, \mu_{t_0|\hat{\boldsymbol{\delta}}^k}) - \frac{x_k - \mu_x}{d_k(\mu_x, \mu_y)}(x - \mu_{x|\hat{\boldsymbol{\delta}}^k}) \\ &- \frac{y_k - \mu_y}{d_k(\mu_x, \mu_y)}(x - \mu_{x|\hat{\boldsymbol{\delta}}^k}) + c(t_0 - \mu_{t_0|\hat{\boldsymbol{\delta}}^k}) \end{aligned} \tag{29}$$

The mean pseudorange used as prior information for base station k is therefore approximated by

$$\mu_{\delta_k} \approx \delta_k(\mu_{x|\hat{\boldsymbol{\delta}}^k}, \mu_{y|\hat{\boldsymbol{\delta}}^k}, \mu_{t_0|\hat{\boldsymbol{\delta}}^k}). \tag{30}$$

The variance of this prior information is by definition given by

$$\sigma_{\delta_k}^2 = \mathcal{E}\{(\delta_k(x, y, t_0) - \mu_{\delta_k})^2\} \tag{31}$$

where operator $\mathcal{E}\{\}$ denotes the statistical expectation.

Using (29) and (30), it results from (31) that this variance can be approximated by

$$\begin{aligned} \sigma_{\delta_k}^2 &\approx \frac{1}{d_k^2(\mu_{x|\hat{\boldsymbol{\delta}}^k}, \mu_{y|\hat{\boldsymbol{\delta}}^k})} \begin{bmatrix} x_k - \mu_{x|\hat{\boldsymbol{\delta}}^k} \\ y_k - \mu_{y|\hat{\boldsymbol{\delta}}^k} \\ -cd_k(\mu_{x|\hat{\boldsymbol{\delta}}^k}, \mu_{y|\hat{\boldsymbol{\delta}}^k}) \end{bmatrix}^T \\ &\cdot \begin{bmatrix} \sigma_{x|\hat{\boldsymbol{\delta}}^k}^2 & \Gamma_{xy|\hat{\boldsymbol{\delta}}^k} & \Gamma_{xt_0|\hat{\boldsymbol{\delta}}^k} \\ \Gamma_{xy|\hat{\boldsymbol{\delta}}^k} & \sigma_{y|\hat{\boldsymbol{\delta}}^k}^2 & \Gamma_{yt_0|\hat{\boldsymbol{\delta}}^k} \\ \Gamma_{xt_0|\hat{\boldsymbol{\delta}}^k} & \Gamma_{yt_0|\hat{\boldsymbol{\delta}}^k} & \sigma_{t_0|\hat{\boldsymbol{\delta}}^k}^2 \end{bmatrix} \cdot \begin{bmatrix} x_k - \mu_{x|\hat{\boldsymbol{\delta}}^k} \\ y_k - \mu_{y|\hat{\boldsymbol{\delta}}^k} \\ -cd_k(\mu_{x|\hat{\boldsymbol{\delta}}^k}, \mu_{y|\hat{\boldsymbol{\delta}}^k}) \end{bmatrix}. \end{aligned} \tag{32}$$

IV. COMPLEXITY AND COMMUNICATION OVERHEAD ANALYSIS

In this section, we analyze the computational complexity of the iterative positioning scheme and compare it to state-of-the-art approaches. We also compare DPE, two-step and iterative positioning approaches in terms of communication overhead.

A. Computational Complexity

We define the computational complexity as the number of real multiplications required to estimate the user position based on the received signals. For the sake of simplicity, we do not consider additions and subtractions since their implementation complexity is negligible compared to multiplications and divisions. The small number of divisions make their impact on the total complexity negligible. We therefore also discard divisions in our analysis. Complex multiplications are assumed to require three real multiplications [28]. To keep the discussion as simple as possible, we assume that grids are used to assess the numerical integrals.

In the following, symbols K and P respectively denote the number of base stations and the number of pilot sub-carriers. N is the number of equispaced points composing both coordinates intervals $[x_{\min}, x_{\max}]$ and $[y_{\min}, y_{\max}]$. The common phase ϕ_k is supposed to be uniformly distributed on $[0, 2\pi[$. We assume a_k to be Rician distributed. Numerical integrals to marginalize the phase and the amplitude in pseudorange estimation and DPE are respectively computed on N_ϕ and N_a points. We also consider integrals on δ_k and t_0 to be computed on N_δ and N_{t_0} points respectively.

1) Direct Positioning Estimation: The DPE scheme considered in this paper is designed according to the MMSE criterion (see Appendix A). It relies on the estimation of the posterior PDF of the user position (46). To compute the numerator of this PDF, the theoretically received signal vector $\mathbf{s}(\delta_k(x, y, t_0))$ is compared to the actually received signal $\mathbf{r}_k$ on the pilot sub-carriers. This involves the multiplication of the two $P \times 1$ complex vectors $\mathbf{r}_k$ and $\mathbf{s}(\delta_k(x, y, t_0))$ for all possible combinations of x, y and t_0. Assuming all the values of $\mathbf{s}(\delta_k(x, y, t_0))$ to be pre-computed and neglecting the impact of the exponential and real part operators, assessing the numerator of (46) requires $3N^2N_{t_0}KP$ real multiplications. Marginalizing the phase ϕ_k and the amplitude a_k and multiplying the K resulting PDFs $p(\mathbf{r}_k|\boldsymbol{\gamma})$ approximately requires $N^2N_{t_0}N_aN_\phi$ real multiplications. Numerical integrals involved in the computation of the denominator of (46) and of the position and clock offset estimator (47) can also be neglected compared to the cost of computing the numerator of (46). We can therefore consider that DPE requires

$$C_{\text{direct}} \approx N^2 N_{t_0} K(3P + N_a N_\phi) \tag{33}$$

real multiplications to determine the user location.

2) Two-step Localization: The two-step position estimation is nearly equivalent to the first iteration of the iterative localization procedure. Each base station first estimates the mean pseudoranges of the received signals together with their reliabilities using the MMSE estimator described in expressions (12) to (14). Building the posterior PDF (12) involves to compute the frequency domain correlation $\mathbf{r}_k^H \cdot \mathbf{s}(\delta_k)$ for all possible values of δ_k. Numerical integrals needed to compute the denominator of (12) and the mean and variance of the pseudorange can be neglected. The impact of the right term of the numerator of (12) linked to the prior pseudorange distribution can also be neglected as well as the exponential and real part operators. Marginalizing the common phase ϕ_k and the amplitude approximately requires $N_a N_\phi N_\delta$ real multiplications for each BS. Estimating the time-of-arrival for the K base stations therefore approximately requires $KN_\delta(3P + N_a N_\phi)$ real multiplications.

The fusion center then deduces the MMSE user position from the K pseudorange estimates using the posterior position PDF (24). The latter PDF needs to be assessed for each possible values of x, y and t_0. Neglecting the cost of numerical integrals involved in expressions (24) to (27), this position estimator approximately requires $N^2N_{t_0}K$ real multiplications. We again neglect the exponential and real part operators in the numerator of (24) and assume that values of $\delta_k(x, y, t_0)$ are pre-computed over the whole parameter grid. This makes the complexity of the MMSE based two-step estimator equal to

$$C_{2s} \approx (N_\delta(3P + N_a N_\phi) + N^2 N_{t_0})K. \tag{34}$$

3) Iterative Localization: Similarly to the two-step estimation, we assume $\mathbf{s}(\delta_k)$ and $\boldsymbol{\delta}_k(x, y, t_0)$ to be pre-computed for all parameter values. For the pseudorange estimation, the term corresponding to the PDF $p(\mathbf{r}_k|\delta_k)$ in (12) can be computed only once and prior to iterating and will therefore only be taken into account at the first iteration. For the next iterations, the dominant terms are the numerical integrals to compute the

mean and variance of the pseudorange estimate. They require approximately KN_δ real multiplications.

Each base station sends its pseudorange estimate together with its reliability to the fusion center where the MS position is estimated. Similar to the two-step case, the posterior PDF (24) is computed for each base station based on the $K - 1$ other stations. Additional operations are also required to compute the mean vector $\boldsymbol{\mu}_{\boldsymbol{\gamma}|\hat{\boldsymbol{\delta}}_k}$ and covariance matrix $C_{\boldsymbol{\gamma}|\hat{\boldsymbol{\delta}}_k}$. Those operations can be neglected compared to the computation of the posterior PDF (24).

The complexity of operations (30) and (32) to convert position informations to a pseudorange information can also be neglected. This leads to a complexity for the MMSE based iterative algorithm equal to

$$\begin{aligned} C_{\text{it}} &\approx N_{\text{iter}}\big(KN^2N_{t_0}(K - 1) + KN_\delta\big) \\ &\quad + KN_\delta(3P + N_a N_\phi) \end{aligned} \tag{35}$$

where N_{iter} denotes the number of iterations.

B. Communication Overhead

If pseudoranges are estimated at the BSs, another advantage of the iterative approach over the DPE is its reduced communication overhead. Considering an uplink positioning scenario, the direct approach indeed requires each base station to transmit its received signal on the pilot sub-carriers to the fusion center. Assuming a N_b bits analogue to digital converter for I and Q branches at each base station, the fusion center should receive

$$b_{\text{direct}} = 2N_b \cdot P \cdot K \tag{36}$$

bits exclusively dedicated to positioning.

For each step of the iterative approach, each base station receives corresponding μ_{δ_k} and $\sigma_{\delta_k}^2$ from the fusion center, estimates the pseudoranges and transmits those estimates $\hat{\delta}_k$ and $\sigma_{e_k}^2$ back to the fusion center. This makes the total number of bits dedicated to positioning equal to

$$b_{\text{it}} = 2N_b \cdot K \cdot (2N_{\text{it}} - 1) \tag{37}$$

where we assumed that mean and variance estimates are represented on N_b bits. N_{it} denotes the number of iterations.

In the two-step approach, the BSs only transmit their pseudorange estimates once to the fusion center. The number of bits dedicated to positioning is therefore

$$b_{2s} = 2N_b \cdot K. \tag{38}$$

Comparing expression (37) to (36) and (38) for 4 BSs, $P = 64$ and $N_{\text{it}} = 6$ iterations yields that the communication overhead of the iterative approach is nine times lower than the DPE but seven times higher than the two-step approach.

V. SIMULATION RESULTS

The following section investigates the performance of the positioning algorithms. We assume a system of four base stations laying at the corners of a 100 m sided square. The MS lies at arbitrary positions in the square and communicates in the uplink with the $K = 4$ BSs at a carrier frequency of 2 GHz.
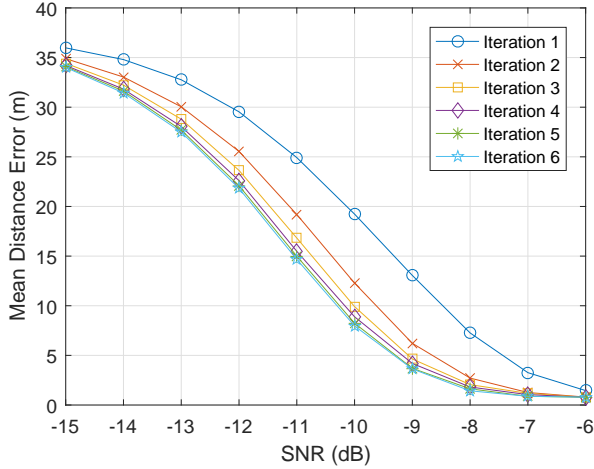
Fig. 2. Convergence of the Iterative Algorithm -
Mean Distance Error as a Function of the Signal-to-Noise Ratio.

The uplink communication uses the OFDM modulation over a bandwidth of 40 MHz. Pilot symbols are spread on $P = 64$ equispaced sub-carriers among 1024. We assume a single path propagation channel. The common phase ϕ_k affecting the received signal in (4) is considered to be uniformly distributed on $[0, 2\pi[$. We consider a strong Line-Of-Sight (LOS) scenario and therefore assume the signal amplitude a_k to be Rician Distributed with a Rice factor of 22dB. Such a Rice factor is used for the first tap of the strong LOS ETSI TDL-E channel model [29]. The Rice factor is assumed to be known by the receiver. The time offset t_0 is randomly drawn from $[0\text{ns}, 250\text{ns}]$. Numerical integrals of the MMSE position estimator are assessed considering that search intervals $[x_{\min}, x_{\max}]$ and $[y_{\min}, y_{\max}]$ are both composed of $N = 70$ equispaced points. The uniform search interval $[t_{0_{\min}}, t_{0_{\max}}]$ is defined on $N_{t_0} = 50$ points. We also consider the interval of possible pseudoranges $[\delta_{\min}, \delta_{\max}]$ to be composed of $N_\delta = 500$ points. The numerical integral to marginalize the common phase ϕ_k and the amplitude a_k are respectively assessed on $N_\phi = 30$ and $N_a = 10$ equispaced points. Those interval lengths are sufficient to make numerical approximations negligible compared to the noise. Algorithm performances depicted in Section V-A are averaged over 500 MS position and noise realizations.

A. Algorithm performance

Figs. 2 illustrates the convergence of the iterative positioning algorithm. This figure depicts the mean distance error as a function of the SNR for an increasing value of the number of iterations. For a given SNR and iteration index, this mean distance error e_d is computed as

$$e_d = \frac{1}{N_{\text{sim}}} \sum_{n=1}^{N_{\text{sim}}} \sqrt{(\hat{x}_n - x_n)^2 + (\hat{y}_n - y_n)^2} \qquad (39)$$

where N_{sim} denotes the number of realizations. Clearly, most of the gain comes from the two first iterations. The algorithm converges after six iterations.

Fig. 3 compares the performance of the iterative algorithm to the two-step and direct localization methods in terms of both average localization and synchronization error as a function of the SNR. The first iteration of the iterative approach is slightly outperformed by the two-step estimation. This is due to the fact that in the two-step case, the position estimate is directly obtained from the pseudoranges of the four BSs while it results from the average of the estimates of the four possible subsets of three BSs in the iterative case. When the number of iterations increases, the performance of the iterative scheme comes closer to the DPE. The mean absolute clock offset error e_{t_0} depicted in Fig.4(b) is computed as

$$e_{t_0} = \frac{1}{N_{\text{sim}}} \sum_{n=1}^{N_{\text{sim}}} \left| \hat{t}_{0n} - t_{0n} \right|. \qquad (40)$$

Multipath propagation: Up to now, only an strong line-of-sight scenario characterized by a single path channel was considered. However, in a cellular environment the signal is often prone to multipath propagation.

A simple scenario to study the impact of multipath propagation on the positioning algorithms is to consider a two-path channel between the MS and BS k given by

$$h_k(t) = e^{j\varphi_k^0} \delta(t - \tau_k) + a_k^1 e^{j\varphi_k^1} \delta(t - \tau_k - \tau_k^1) \qquad (41)$$

where a_k^1, φ_k^1 and τ_k^1 are respectively the amplitude, the phase and the delay of the reflection. We assume the first path to be affected by a phase φ_k^0. Fig. 4 illustrates the impact of this multipath reflection on our positioning algorithm. The pilot signal is subject to the multipath channel (41) with a_k^1 chosen to have a Signal to Multipath Ratio (SMR) of 1 dB and a reflection delay τ_k^1 randomly chosen in the uniform interval $[0, \tau_{\max}^1]$. The phases φ_k^0 and φ_k^1 are randomly drawn from the uniform interval $[0, 2\pi[$. Fig. 4 shows that the multipath reflection actually acts as an additional noise component. The distance error and synchronization error curves are shifted to the right by 1 dB for the direct, the two-step and iterative methods after convergence. There is also a saturation effect at high SNR, i.e. the multipath reflection introduces a noise floor in the positioning process.

Obstructed LOS propagation: When the LOS between MS and BS is obstructed as often occurs in indoor and urban environments, the time-of-arrival of the strongest path is affected by a positive bias compared to the LOS propagation time τ_k. We therefore investigate the impact of obstructed-line-of-sight (OLOS) errors on the positioning algorithms by including a random bias $t_{bk} \sim U[0, t_{b\max}]$ in the observed signal ToA at base station k

$$t_k = \tau_k(x, y) + t_0 + t_{bk}. \qquad (42)$$

Figs. 5(a) and 5(b) respectively illustrate the distance and synchronization errors as a function of the SNR when the ToAs are affected by OLOS errors as in equation (42). Each base station is affected by an independent time bias t_{bk} randomly drawn from the uniform interval $[0, t_{b\max}]$ with $t_{b\max} = 45$ ns. This maximum bias of 45 ns corresponds to the delay of the strongest path of the NLOS Tapped Delay Line A (TDL-A) channel model of the 3GPP Urban Microcell (3GPP UMi)
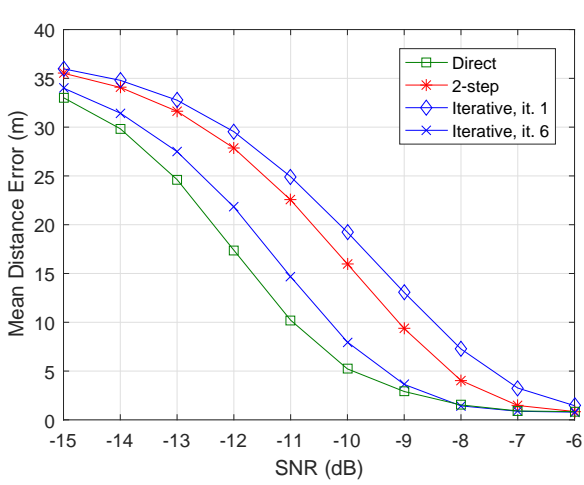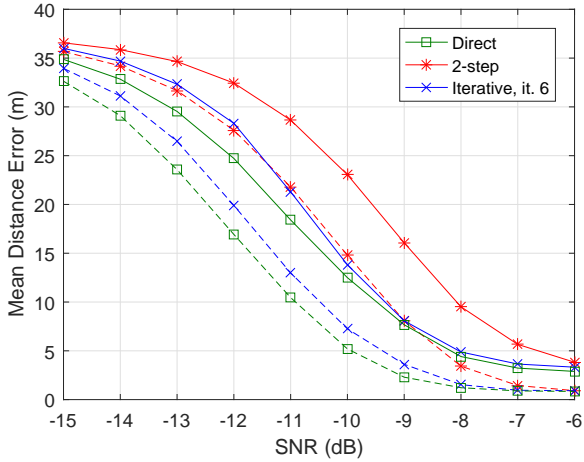
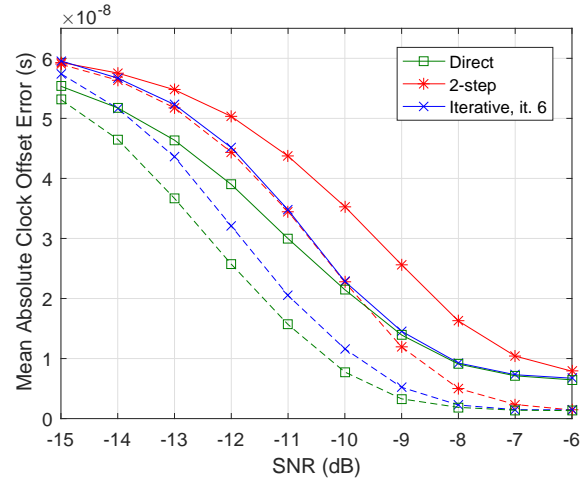(a) Mean Distance Error as a Function of the Signal-to-Noise Ratio
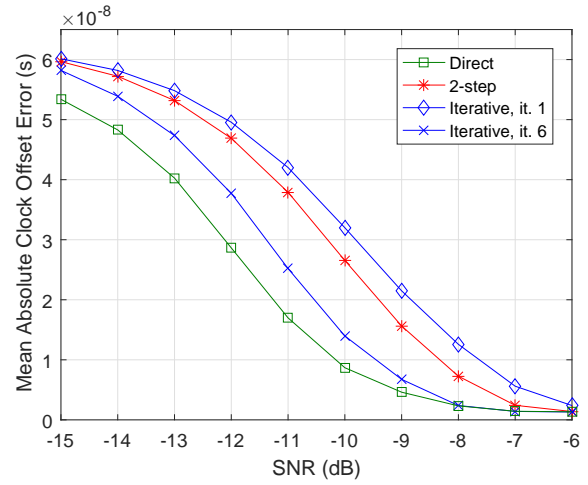
(b) Mean Absolute Clock Offset Error as a Function of the Signal-to-Noise Ratio.

Fig. 3. Performance of the Positioning Algorithms.

(a) Mean Distance Error as a Function of the Signal-to-Noise Ratio

(b) Mean Absolute Clock Offset Error as a Function of the Signal-to-Noise Ratio

Fig. 4. Effect of a Multipath Reflection on the Positioning Algorithms. Solid line: 2-paths Channel (41), SMR = 1dB, $\tau_{\max}^1 = 35$ns. Dashed Line: Single Path Propagation, signal amplitude fixed to $a_k = 1$.

Street-Canyon scenario [29], considering a channel delay spread of 120 ns. According to Table 7.7.3-2 in [29], 120 ns corresponds to a normal delay spread for this NLOS UMi scenario for a 2 GHz carrier frequency. Fig. 5 shows that at low to medium SNR, the performance of the iterative algorithm is degraded compared to the pure LOS case but the performance after six iterations is still improved compared to the two-step approach since noise dominates the impact of OLOS errors. At high SNR, OLOS errors dominate the noise and the iterative as well as the direct positioning methods perform slightly worse than the two-step localization. Observations are similar for the synchronization performance. However, the relative impact of the OLOS propagation bias is more pronounced at high SNR than for the positioning.

B. Complexity comparison

Fig. 6 illustrates the number of cumulated real multiplications for the iterative algorithm compared to the two-step and direct positioning approaches. Those curves are drawn from the complexity formulas (33) to (35). The iterative algorithm is five times more complex than the two-step approach from the first iteration. This is due to the fact that the position estimator must be run for each base station in the iterative case and only once for the two-step approach. Assessing position and time offset (co)variances also induces a complexity increase.

It should also be noted that if the pseudorange estimation is performed at the BSs, the DPE approach concentrates the computing effort on the fusion center while the two-step and iterative approaches share the computations between the BSs that estimate the time of arrivals and the fusion center that deduces the position estimate.
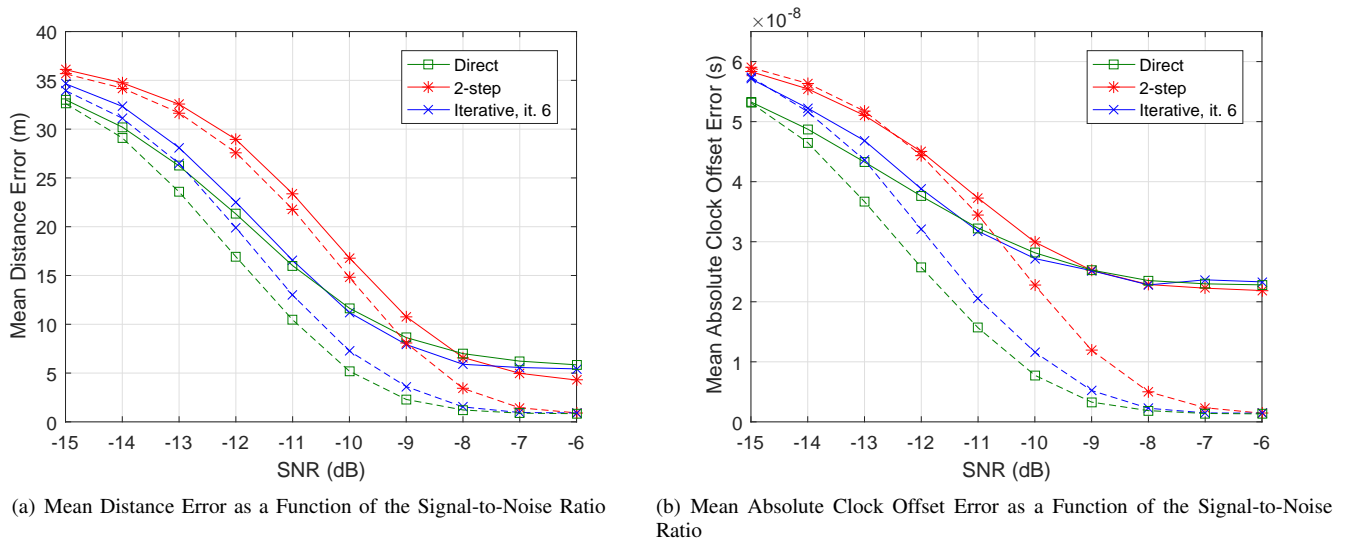
(a) Mean Distance Error as a Function of the Signal-to-Noise Ratio

(b) Mean Absolute Clock Offset Error as a Function of the Signal-to-Noise Ratio

Fig. 5. Effect of OLOS Propagation Errors on the Positioning Algorithms. Solid Line: OLOS Propagation, $t_{b\max} = 45$ns. Dashed Line: Strong LOS Single Path Propagation, $t_{bk} = 0$ s, signal amplitude fixed to $a_k = 1$.
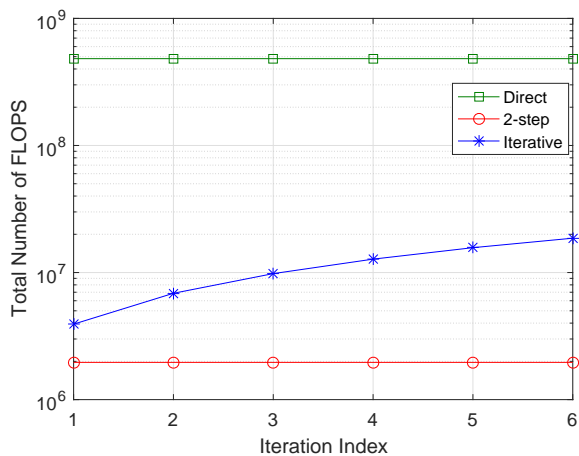

Fig. 6. Comparison of the Computational Complexity of the Two-step, Iterative and Direct Positioning Algorithms. Cumulated Number of Real Multiplications as a Function of the Iteration Index.

VI. CONCLUSION

In this paper, we propose an iterative joint positioning and synchronization algorithm able to operate in a cellular system where the MS is only roughly time synchronized to the connected BSs. This algorithm refines the position estimate traditionally acquired in two steps by iterating between the pseudorange and position estimation steps. Pseudorange and position estimates are exchanged together with an indication of their reliability between the two steps. The position and time offset computed during a pass of the algorithm are translated to a pseudorange information used as prior information by the next iteration. This allows to progressively recover the information contained in the received signal that is discarded by the two-step approach.

We illustrate using numerical simulations that the iterative localization system approaches the performance of the direct positioning algorithm while reducing the computational load by one order of magnitude.

APPENDIX A
DIRECT POSITIONING ALGORITHM

The direct positioning localization scheme used in this paper is inspired from [30]. It relies on a MMSE estimation implemented making use of the Bayes framework to take into account some available prior information. Paper [30] develops a MMSE direct positioning algorithm to perform a sequential tracking of the position of the MS based using a motion model. We rather reformulate the estimator for static positioning, using as prior information the distribution of the user position and time offset.

Assuming that each BS makes an independent position estimation, we have

$$p(\mathbf{r}_1, ..., \mathbf{r}_K | \boldsymbol{\gamma}) = \prod_{k=1}^{K} p(\mathbf{r}_k | \boldsymbol{\gamma}) \tag{43}$$

where $\boldsymbol{\gamma} = [x, y, t_0]^T$ and

$$p(\mathbf{r}_k | \boldsymbol{\gamma}) = \int_{-\infty}^{+\infty} \int_{-\infty}^{+\infty} p(\mathbf{r}_k | \boldsymbol{\gamma}, a_k, \phi_k) p(a_k) p(\phi_k) da_k d\phi_k \tag{44}$$

The joint posterior distribution of the positioning parameters for all base stations can be expressed following the Bayesian framework as

$$p(\boldsymbol{\gamma} | \mathbf{r}_1, ..., \mathbf{r}_K) = \frac{p(\mathbf{r}_1, ..., \mathbf{r}_K | \boldsymbol{\gamma}) p(\boldsymbol{\gamma})}{\int_{-\infty}^{+\infty} p(\mathbf{r}_1, ..., \mathbf{r}_K | \boldsymbol{\gamma}) p(\boldsymbol{\gamma}) d\boldsymbol{\gamma}}. \tag{45}$$

We deduce from (4) that $\mathbf{r}_k$ follows a Gaussian distribution. Assuming in addition that $\boldsymbol{\gamma}$ is uniformly distributed on interval $[\boldsymbol{\gamma}_{\min}, \boldsymbol{\gamma}_{\max}]$, the posterior PDF (45) can be written after some simplification as expression (46).

$$p(\boldsymbol{\gamma}|\mathbf{r}_1, ..., \mathbf{r}_K) = \frac{\prod_{k=1}^{K}\left(\int\limits_{-\infty}^{+\infty}\int\limits_{-\infty}^{+\infty}\exp\left(\frac{2}{\sigma_{w_k}^2}a_k\cos\phi_k\Re\{\mathbf{r}_k^H\cdot\mathbf{s}\left(\delta_k(\boldsymbol{\gamma})\right)\}-a_k^2P\right)p(a_k)p(\phi_k)da_kd\phi_k\right)}{\int\limits_{\boldsymbol{\gamma}_{\min}}^{\boldsymbol{\gamma}_{\max}}\prod_{k=1}^{K}\left(\int\limits_{-\infty}^{+\infty}\int\limits_{-\infty}^{+\infty}\exp\left(\frac{2}{\sigma_{w_k}^2}a_k\cos\phi_k\Re\{\mathbf{r}_k^H\cdot\mathbf{s}\left(\delta_k(\boldsymbol{\gamma})\right)\}-a_k^2P\right)p(a_k)p(\phi_k)da_kd\phi_k\right)d\boldsymbol{\gamma}} \tag{46}$$

Numerically computing the mean of $\boldsymbol{\gamma}$ provides the MMSE estimate of the position and of the clock offset

$$\hat{\boldsymbol{\gamma}} = \int\limits_{\boldsymbol{\gamma}_{\min}}^{\boldsymbol{\gamma}_{\max}} \boldsymbol{\gamma}\, p(\boldsymbol{\gamma}|\mathbf{r}_1, ..., \mathbf{r}_K)d\boldsymbol{\gamma}. \tag{47}$$

REFERENCES

[1] R. S. Campos, "Evolution of positioning techniques in cellular networks, from 2G to 4G," *Wireless Communications and Mobile Computing*, vol. 2017, 2017.

[2] C. Cox, *An Introduction to LTE: LTE, LTE-Advanced, SAE and 4G Mobile Communications.* Wiley, 2012.

[3] R. Zekavat and R. M. Buehrer, *Source Localization: Algorithms and Analysis.* Wiley-IEEE Press, 2012, pp. 25–66.

[4] R. M. Vaghefi and R. M. Buehrer, "A linear estimator for joint synchronization and localization in wireless sensor networks," in *IEEE Global Commun. Conf. (GLOBECOM)*, Dec 2014, pp. 505–510.

[5] K. Cheung, H. So, W.-K. Ma, and Y. Chan, "A constrained least squares approach to mobile positioning: Algorithms and optimality," *EURASIP J. Adv. in Signal Process.*, vol. 2006, no. 1, p. 020858, 2006.

[6] M. Sun and L. Yang, "On the joint time synchronization and source localization using ToA measurements," *Int. J. Distributed Sensor Networks*, vol. 9, no. 2, p. 794805, 2013.

[7] J. Zheng and Y. C. Wu, "Joint time synchronization and localization of an unknown node in wireless sensor networks," *IEEE Trans. Signal Process.*, vol. 58, no. 3, pp. 1309–1320, Mar 2010.

[8] W. Wang, T. Jost, and U. Fiebig, "Characteristics of the NLoS Bias for an Outdoor-to-Indoor Scenario at 2.45 GHz and 5.2 GHz," *IEEE Antennas and Wireless Propagation Letters*, vol. 10, pp. 1127–1130, 2011.

[9] J.-Y. Lee and R. A. Scholtz, "Ranging in a dense multipath environment using an UWB radio link," *IEEE J. on Select. Areas Commun.*, vol. 20, no. 9, pp. 1677–1683, Dec 2002.

[10] X. Li and K. Pahlavan, "Super-resolution TOA estimation with diversity for indoor geolocation," *IEEE Trans. Wireless Commun.*, vol. 3, no. 1, pp. 224–234, Jan 2004.

[11] R. Roy and T. Kailath, "ESPRIT-estimation of signal parameters via rotational invariance techniques," *IEEE Trans. Acoust., Speech, Signal Process.*, vol. 37, no. 7, pp. 984–995, Jul 1989.

[12] O. Bialer, D. Raphaeli, and A. J. Weiss, "Efficient Time of Arrival Estimation Algorithm Achieving Maximum Likelihood Performance in Dense Multipath," *IEEE Trans. Signal Process.*, vol. 60, no. 3, pp. 1241–1252, Mar 2012.

[13] ——, "Robust time-of-arrival estimation in multipath channels with OFDM signals," in *25th European Signal Process. Conf.*, Aug 2017, pp. 2724–2728.

[14] I. Guvenc and C. C. Chong, "A Survey on TOA Based Wireless Localization and NLOS Mitigation Techniques," *IEEE Commun. Surveys Tutorials*, vol. 11, no. 3, pp. 107–124, rd 2009.

[15] H. Chen, G. Wang, Z. Wang, H. C. So, and H. V. Poor, "Non-Line-of-Sight Node Localization Based on Semi-Definite Programming in Wireless Sensor Networks," *IEEE Trans. Wireless Commun.*, vol. 11, no. 1, pp. 108–116, Jan 2012.

[16] P. Closas, C. Fernandez-Prades, and J. A. Fernandez-Rubio, "Maximum likelihood estimation of position in GNSS," *IEEE Signal Process. Lett.*, vol. 14, no. 5, pp. 359–362, May 2007.

[17] N. Vankayalapati, S. Kay, and Q. Ding, "TDoA based direct positioning maximum likelihood estimator and the Cramer-Rao bound," *IEEE Trans. Aerosp. Electron. Syst.*, vol. 50, no. 3, pp. 1616–1635, July 2014.

[18] A. Amar and A. J. Weiss, "New asymptotic results on two fundamental approaches to mobile terminal location," in *3rd Int. Symp. Commun., Control and Signal Process.*, Mar 2008, pp. 1320–1323.

[19] P. Closas, C. Fernandez-Prades, and J. A. Fernandez-Rubio, "Direct position estimation approach outperforms conventional two-steps positioning," in *2009 17th European Signal Process. Conf.*, Aug 2009, pp. 1958–1962.

[20] O. Bar-Shalom and A. J. Weiss, "Direct position determination of OFDM signals," in *IEEE 8th Workshop Signal Process. Advances Wireless Commun.*, June 2007, pp. 1–5.

[21] Z. Lu, J. Wang, B. Ba, and D. Wang, "A Novel Direct Position Determination Algorithm for Orthogonal Frequency Division Multiplexing Signals Based on the Time and Angle of Arrival," *IEEE Access*, vol. 5, pp. 25 312–25 321, 2017.

[22] M. Wax and T. Kailath, "Decentralized processing in sensor arrays," *IEEE Trans. Acoust., Speech, Signal Process.*, vol. 33, no. 5, pp. 1123–1129, Oct 1985.

[23] P. Stoica, A. Nehorai, and T. Söderström, "Decentralized array processing using the MODE algorithm," *Circuits, Syst. Signal Process.*, vol. 14, no. 1, pp. 17–38, Jan 1995.

[24] F. Horlin, M. Van Eeckhaute, T. Van der Vorst, A. Bourdoux, F. Quitin, and P. De Doncker, "Iterative ToA-based Terminal Positioning in Emerging Cellular Systems," in *IEEE Int. Conf. Commun. (ICC)*, May 2017.

[25] C. Mensing, "Location determination in ofdm based mobile radio systems," Dissertation, Technische Universitat Munchen, Munchen, 2013.

[26] S. Ahmadi, *LTE-Advanced: A Practical Systems Approach to Understanding 3GPP LTE Releases 10 and 11 Radio Access Technologies*, ser. EngineeringPro collection. Elsevier Science, 2013.

[27] S. Kay, *Fundamentals of Statistical Signal Processing: Detection theory*, ser. Prentice Hall Signal Processing Series. Prentice-Hall PTR, 1993.

[28] D. E. Knuth, *The Art of Computer Programming, Volume 2 (3rd Ed.): Seminumerical Algorithms.* Boston, MA, USA: Addison-Wesley Longman Publishing Co., Inc., 1997.

[29] "5G; Study on channel model for frequencies from 0.5 to 100 GHz," 3rd Generation Partnership Project (3GPP), TR 38.901 V14.0.0, May 2017. [Online]. Available: http://www.etsi.org/deliver/etsi_tr/138900_138999/138901/14.00.00_60/tr_138901v140000p.pdf

[30] P. Closas, C. Fernandez-Prades, D. Bernal, and J. A. Fernandez-Rubio, "Bayesian direct position estimation," in *Proc. 21st ION GNSS 2008*, Sept 2008, pp. 183–190.

Mathieu Van Eeckhaute received the M.Sc. degree in electrical engineering from the Université Libre de Bruxelles (ULB), Brussels, Belgium, in 2016. Since September 2016, he is a Ph.D. student working at OPERA WCG, Université libre de Bruxelles. From July 2015 to June 2016, he participated in a research project in collaboration with the Interuniversity microelectronics centre (IMEC) in Leuven, Belgium, to perform a survey study on emerging multicarrier waveforms for 5G. His research activities currently focus on terminal positioning based on new 5G waveforms and on the impact of the wireless communication channel on time-of-arrival and time-difference-of-arrival localization schemes.

Thomas Van der Vorst received the M.Sc. degree in physics engineering from the Université Libre de Bruxelles (ULB), Brussels, Belgium, in 2016. Since September 2016, he is a Ph.D. student working part time at OPERA WCG, Université libre de Bruxelles and at Laboratoire d'Electronique et Electromagnétisme, Sorbonne Université, Paris, France. His research interests focus on angle-of-arrival based localization for the Internet-of-Things.

François Horlin received the Ph.D. degree from the Université Catholique de Louvain, Louvain-La-Neuve, Belgium, in 2002. He specialized in the field of signal processing for digital communications. He joined the Interuniversity Micro-Electronics Center in 2002. He led the project aiming at developing a 4G cellular communication system in collaboration with Samsung Korea. In 2007, he became a Professor at the Université Libre de Bruxelles (ULB), Brussels, Belgium. He is currently supervising a research team working on next-generation communication systems. Localization based on 5G signals, filterbank-based modulations, massive multiple input and multiple output, and dynamic spectrum access are examples of currently investigated research topics. He has been academic representative to the executive board of ULB from 2010 to 2015. Since 2017, he has been the Vice Dean for research with the Ecole Polytechnique de Bruxelles.

André Bourdoux received the M.Sc. degree in electrical engineering in 1982 from the Université Catholique de Louvain, Louvain-la-Neuve, Belgium. He joined IMEC in 1998 and is a Principal Scientist with the Perceptive Systems for the IoT Department of IMEC. He is a system level and signal processing expert for both the wireless communications and radar teams. He has 10 years of research experience in radar systems and 15 years of research experience in wireless. He holds several patents in these fields. He is the author and coauthor of more than 140 publications in books and peer-reviewed journals and conferences.

François Quitin received the Ph.D. degree in electrical engineering from the Université Libre de Bruxelles (ULB), Brussels, Belgium, and the Université Catholique de Louvain, Louvain-La-Neuve, Belgium, in 2011. He is an Assistant Professor with the ULB. From 2011 to 2013, he was a Postdoctoral Researcher with the University of California, Santa Barbara, and from 2013 to 2015, he was a Postdoctoral Research Fellow with Nanyang Technological University, Singapore. His research interests include experimental and prototyping aspects in wireless communications, taking advanced theoretical ideas all the way to practice. He received the Alcatel-Lucent Bell Scientific Award in 2012.

Philippe De Doncker received the M.Sc. degree in physics engineering and the Ph.D. degree in science engineering from the Université Libre de Bruxelles (ULB), Brussels, Belgium, in 1996 and 2001, respectively. He is currently a Professor with the ULB, where he leads the research activities on wireless channel modeling and (bio)electromagnetics.